

Supporting Information

Methods

Materials. Natural graphite flakes (NG, 7.94 m²/g, Canrd Co. Ltd.), spherical graphitized mesocarbon microbeads (MCMB, 2.25 m²/g, Canrd Co. Ltd.) and coconut shell derived activated carbon (AC, 1000~1200 m²/g, Green activated carbon Co. Ltd.) were used as the active materials without further treatment. Electrolyte solutions were prepared by dissolving zinc salts in pure water to target molar ratios. Both ZnCl₂ (purity 99.95%) and ZnBr₂ (purity 99.9%) were purchased from Shanghai Macklin Biochemical Co. Ltd.

Cell fabrications. Electrodes were prepared by pressing the powder mixture of 3 mg of active material and 2 mg of conductive binder (teflonized acetylene black, Denka Co., Ltd.) on a titanium sheets (Hefei Kejing Materials Technology Co. Ltd., $\phi=14$ mm). Every Swagelok cell (with Ti pillars) contains a Zn negative electrode, a positive electrode (dried at 130 °C under vacuum for 3 h before use) two pieces of separators (glass fiber (Whatman GF/A 1820) soaked by 170 μ L of electrolyte solutions. All cells were assembled in the air.

Electrochemical Measurements. Galvanostatic charge-discharge were performed by the Neware battery test system (CT-4008-10V50mA, Shenzhen, China, NEWARE Co. Ltd.). Cyclic voltammetry tests were carried out by a CHI 660E electrochemical work station. Electrochemical impedance spectra (EIS) were measured by Multi Autolab M204 (Metrohm) with a 5 mV amplitude in the range of 0.01~1MHz.

Characterizations. X-ray diffraction (XRD) measurements were taken by a Rigaku MiniFlex600 X-ray diffractometer with Cu K α radiation (20 kV, $\lambda = 1.5418$ Å) between 15~45 ° under 5 °/min. SEM images were obtained on a JSM-7100F scanning electron microscope (JEOL, Japan). *In-situ* Raman spectroscopic tests were achieved by SPELEC RAMAN LASER Class 3B (the laser wavelength was 785 nm) at a scanning rate of 0.1 mV s⁻¹. ¹H-NMR spectra were recorded on a Bruker Av400NMR spectrometer.

Unless specified, the potential windows were 1~2 V (vs. Zn/Zn²⁺) and the ambient temperature were 25°C.

Molecular dynamic (MD) simulations. ZnCl₂@ZnBr₂ electrolytes and ZnCl₂@ZnBr₂ electrolyte-electrode systems were respectively investigated by molecular dynamic (MD) simulation. The pristine ZnCl₂@ZnBr₂ aqueous solution was composed of 200 ZnCl₂, 86 ZnBr₂ and 400 H₂O packed into one cubic simulation box with size of 34.88 Å. The theoretical computation density of ZnCl₂@ZnBr₂ aqueous solution is 2.106 g/cm³. Another ZnCl₂@ZnBr₂ aqueous solution containing 447 ZnCl₂, 192 ZnBr₂ and 894 H₂O was sandwiched by graphite or amorphous carbon coating (ACC) graphite and Zn electrode, denoted by graphite/ZnCl₂@ZnBr₂ electrolyte/Zn and ACC graphite/ZnCl₂@ZnBr₂ electrolyte/Zn systems. The dimensional lengths are 36.28 Å \times 37.71 Å \times 140.0 Å for graphite/ ZnCl₂@ZnBr₂ electrolyte/Zn system, and 36.28 Å \times 37.71 Å \times 155.0 Å for ACC graphite/ ZnCl₂@ZnBr₂ electrolyte/Zn system. There exit two vacuums of each larger than 30 Å at outside of two electrodes. The scenarios of charged graphite and ACC graphite were also considered. In detail, the top layer of graphite electrode was charged by 0.1 C/m², and the amorphous carbon and top layer of graphite was charged by 0.0738 C/m². All MD simulations were carried out by Forcite module with COMPASS II force field ^{1,2} in MS. Van der Waals and Coulomb interactions were respectively considered by atom based and Ewald methods with a cut-off value of 15.5 Å. Equations of motion were integrated with a time step of 1 fs. After energy minimization, each system was fully relaxed under periodic boundary conditions for 400 ps in the NVT (T = 298.0 K) ensemble using the Nose thermostat, which was long enough for system temperature, potential and total energy to get

stable. The MD trajectories were outputted at an interval of 4 ps for radial distribution function (RDF) and density distribution analysis. The coordination number N_i of particles i in the first solvation shell surrounding center atoms was calculated as:

$$N_i = 4\pi\rho$$

in which R_M is the distance of the first minimum following the first peak in the RDF $g(r)$ and ρ is the number density of particles i . The binding energies E_b between electrolyte and electrode were calculated according to the following equation:

$$E_b = E_{total} - E_{electrolyte} - E_{electrode}$$

Where E_{total} is the total energy of electrolyte-electrode system, and $E_{electrolyte}$ and $E_{electrode}$ are the energies of electrolyte and electrode, respectively.

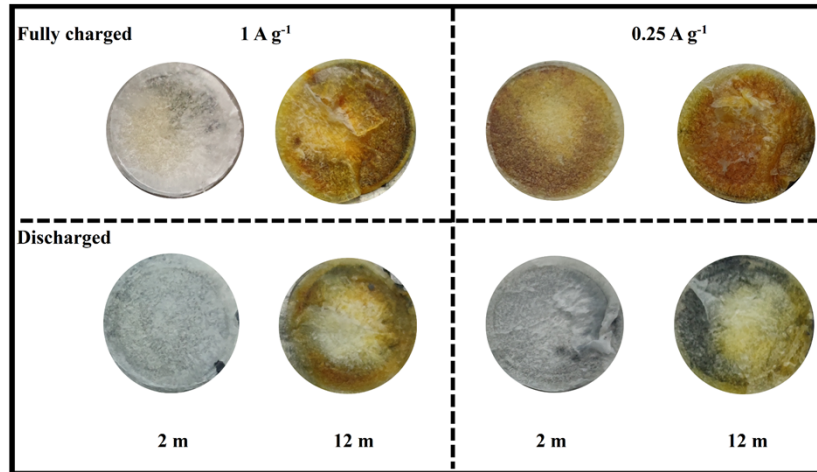


Figure S1. Separators clinging disassembled from the tested Zn/NG batteries.

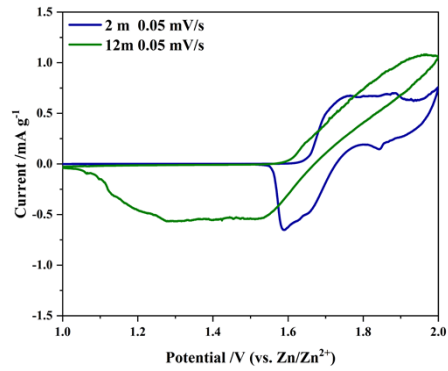


Figure S2. Cyclic voltammograms of NG electrodes using electrolytes of 2m and 12m.

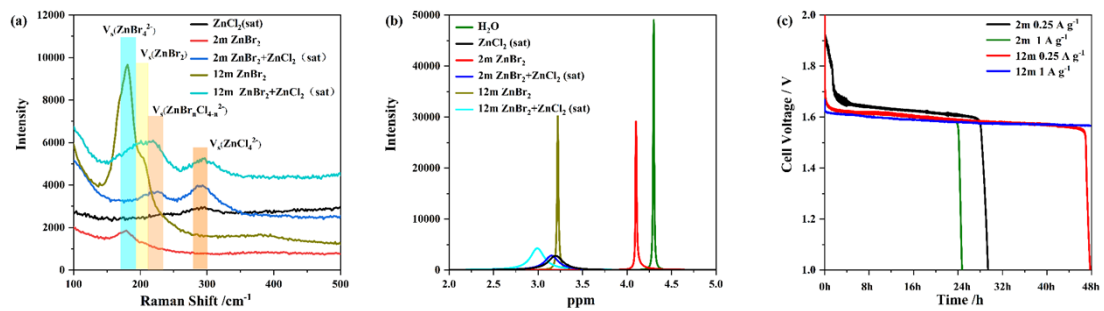


Figure S3. (a) Raman spectra and (b) $^1\text{H-NMR}$ patterns of electrolyte solutions. (c) Self-discharging curves of charged Zn/NG batteries.

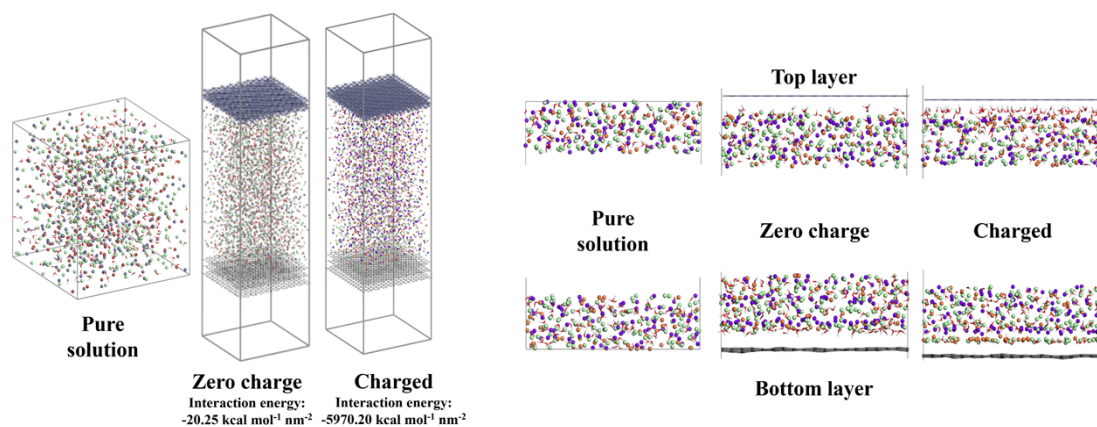


Figure S4. Last snapshots of MD simulated 12 m ZnBr_2 dissolved in saturated ZnCl_2 solution.

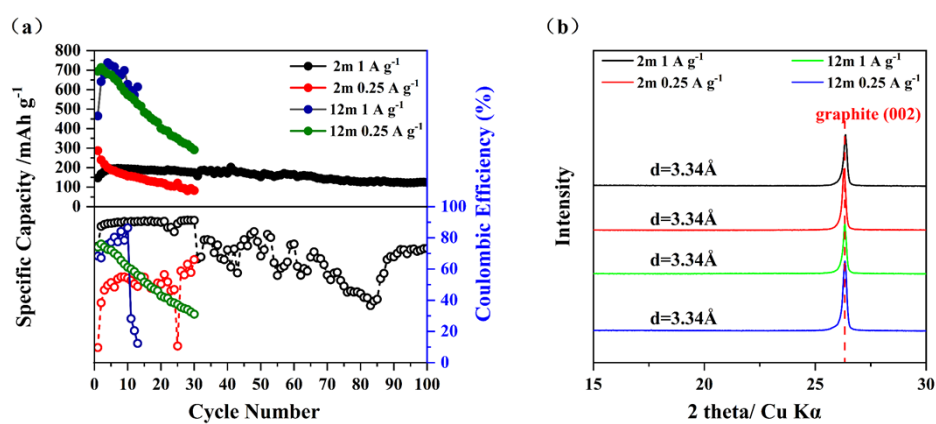


Figure S5. (a) Cycling performances of NG electrodes under different current densities. (b) XRD patterns of NG electrodes after cycling.

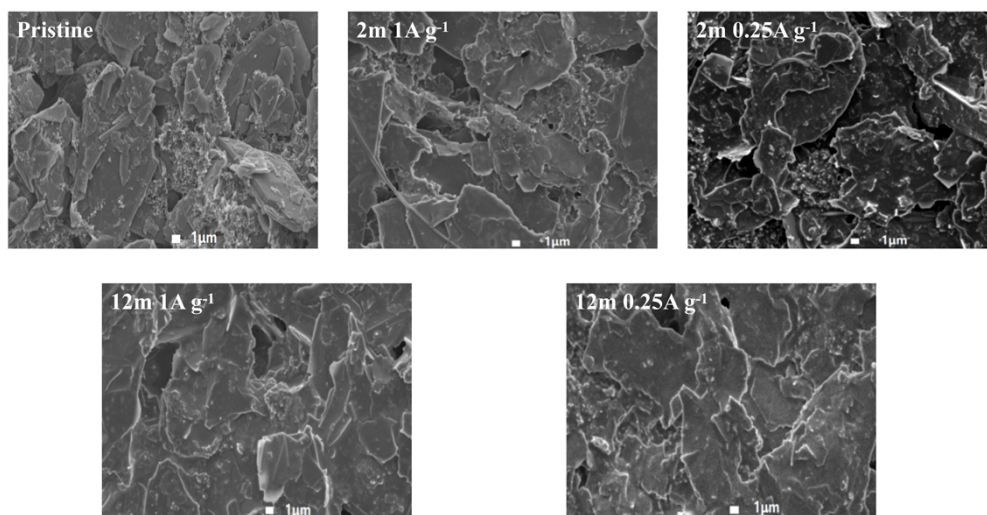


Figure S6. SEM images of NG electrode before and after cycling tests.

References

1. H. Sun, P. Ren and J. R. Fried, *Computational and Theoretical Polymer Science*, 1998, **8**, 229-246.
2. H. Sun, *The Journal of Physical Chemistry B*, 1998, **102**, 7338-7364.
3. O. Borodin, M. Olguin, P. Ganesh, P. R. C. Kent, J. L. Allen and W. A. Henderson, *Physical Chemistry Chemical Physics*, 2016, **18**, 164-175.
4. Y. Wang, X. Huang and X. Zhang, *Nature Communications*, 2021, **12**, 1291.